JOURNAL OF CATALYSIS 153, 41–53 (1995)

The Effects of Bulk Titania Crystal Structure on the Adsorption and Reaction of Aliphatic Alcohols

Victor S. Lusvardi,* Mark A. Barteau,*,[1,2] and William E. Farneth†

*Center for Catalytic Science and Technology, Department of Chemical Engineering, University of Delaware, Newark, Delaware 19716; and †Central Research and Development Department, E.I. duPont de Nemours & Company, Wilmington, Delaware 19880

Received June 20, 1994; revised December 1, 1994

Previous studies on TiO_2 (rutile) single-crystal surfaces have suggested that product distributions in the reactions of primary alcohols and carboxylic acids are governed primarily by the coordination environment of individual surface cations. Since the cation coordination environment is the same in both the anatase and rutile bulk structures, this model would suggest that the reactivity of adsorbed alcohols should be insensitive to bulk structure. In order to test this hypothesis, methanol, ethanol, and 2-propanol were adsorbed at room temperature on TiO_2 anatase and rutile powders. Temperature-programmed desorption spectra were obtained in a high-vacuum microbalance system. On rutile, the molecular coverage was equal for methanol and ethanol but decreased for 2-propanol, most likely due to steric effects observed in previous comparisons of the saturation coverages of primary and secondary alcohols on anatase. The alcohols were dissociatively adsorbed to form alkoxides and surface hydroxyls. The alkoxide species were removed via two channels, recombination with surface hydroxyls at approximately 400 K and decomposition at higher temperatures. The high-temperature decomposition products were identical on both powders, with some differences in the product selectivity. Dehydration and dehydrogenation pathways were observed for all of the alcohols, with only the primary alcohols yielding bimolecular reaction products. The similarities in product distribution and peak temperatures from the aliphatic alcohols on anatase and rutile, particularly with regard to the selectivity for diethyl ether formation from ethanol, indicate that the bulk crystal structure of the oxide does not have a significant influence on the reactions of these molecules. The small differences in selectivity observed between anatase and rutile may be attributed to different populations of coordinatively unsaturated Ti cations on the surfaces of the two powders. However, the reactivity of both high-surface-area anatase and rutile can be understood in terms of the surface site requirements deduced from experiments on rutile single crystals.

INTRODUCTION

Anatase and rutile are polymorphic forms of titania and have been the subject of many surface chemical studies. Both forms possess a 6–3 configuration, with each titanium cation coordinated to six oxygen anions in a slightly distorted octahedron, and each oxygen coordinated to three titanium cations in a nearly equilateral triangle (1). The main difference between the anatase (tetragonal, $I4_1/amd$) and rutile (tetragonal, $P4_2/mnm$) structures is in the packing of these octahedra. Anatase powders are metastable at all temperatures and transform to rutile upon heating (2). The anatase-to-rutile transition temperature has previously been shown to be a function of impurity content, particle size, and surface area (3). The transformation of spectroscopically pure anatase to rutile is immeasurably slow below 883 K, but it proceeds rapidly at temperatures in excess of 1000 K (3–5). The surface areas of anatase powders are typically greater than those of rutile powders, and therefore anatase is preferred as a catalyst support in applications such as titania-supported vanadia catalysts for selective catalytic reduction (SCR) of NO_x with NH_3. In contrast, surface science studies of titania single crystals have generally focused on the more stable rutile form, and the applicability of these results to high-surface-area anatase is uncertain.

Studies of the adsorption and reaction of oxygenated compounds on anatase and rutile have often attributed differences in the adsorption properties and catalytic activity to the different bulk crystal structures (6–10). The comparison of anatase and rutile is challenging since many factors may influence the surface structure of the titania powder.

Studies performed on well-defined single crystals allow for the direct determination of the role of surface structure on reactivity. The adsorption and decomposition of methanol was studied on a rutile single crystal with the {011}-faceted and {114}-faceted (001) surfaces exposed (11). The {114}-faceted (001) surface, which exposes four-, five-, and sixfold coordinated cations (12, 13) evolved dimethyl ether, while the {011}-faceted (001) surface, which exposes five- and sixfold coordinated cations, did not produce detectable quantities of dimethyl ether. The {011}-faceted (001) surface also produced no ethers from higher alcohols

[1] To whom all correspondence should be addressed.
[2] E-mail address: barteau@che.udel.edu.

0021-9517/95 $6.00

(14). These observations form the basis for the conclusion that the reactivity of alcohols is a function of the local cation coordination environment. A similar difference was observed in the reactions of carboxylic acids on these surfaces; bimolecular ketonization of higher carboxylates was observed only on the {114}-faceted (001) surface (15, 16). For formic acid, the analogous bimolecular reaction produces formaldehyde on the {114}-faceted but not the {011}-faceted (001) surface(17). Onishi *et al.* reported no formaldehyde production from formic acid on a rutile single crystal with the (110) surface, which only exposes five- and sixfold coordinated cations (18). It was therefore concluded that these bimolecular reactions, ether formation from surface alkoxides and ketone formation from carboxylates, require individual surface cations with a pair of coordination vacancies, in order to accommodate the two ligands to be coupled at a common cation (11, 15).

In this paper we test the applicability of these ideas to reactions of alcohols on polycrystalline powders. The test involves two implications of the model. First, since cation coordination environments on rutile powders that have not been strongly reduced should be limited to four-, five-, and sixfold coordination, one would expect a similar product distribution to that observed on a rutile single crystal with the {114}-faceted (001) surface exposed (11). Second, since rutile and anatase have similar bulk coordination, one would expect similar selectivities on polycrystalline samples of the two polymorphs for reactions controlled by cation coordination environment.

We have therefore compared the adsorption and reaction of three aliphatic alcohols, methanol, ethanol, and 2-propanol, on anatase and rutile powders. The decomposition of aliphatic alcohols on both materials produced a complex slate of reaction products, which included those of dehydration, dehydrogenation, hydrogenation, and carbonyl coupling reactions. However, the reaction kinetics and selectivities for these various pathways were quite similar on the two polymorphs, as one would expect if these were influenced primarily by local surface cation coordination environment. Also, site requirements for unimolecular and bimolecular reactions of alcohols, deduced from studies performed on rutile single crystals, were completely consistent with the observed reaction products on polycrystalline samples of both titania polymorphs.

EXPERIMENTAL

Chemisorption and temperature-programmed desorption (TPD) of alcohols on titania were studied in a high-vacuum system. The system was pumped with a CTI-Cryotorr 8 cryogenic pump and the typical background pressure was ca. 5×10^{-9} Torr. Adsorption data were obtained gravimetrically on a Cahn RG microbalance (1 μg resolution; sample mass 50–300 mg) within the vacuum system. Gases were admitted into the microbalance chamber through an attached manifold. Pressure within the microbalance chamber was monitored with a Baratron capacitance manometer. TPD spectra were obtained by monitoring the effluent gas stream from the microbalance chamber with a UTI 100C quadrupole mass spectrometer. The heating rate was 5 K/min. Details of this apparatus have been described previously (19, 20).

Alcohol reagents were subjected to three freeze–pump–thaw cycles prior to use. Anatase powder was purchased from Fisher-Scientific, and the rutile powder was provided by E. I. DuPont de Nemours & Co., Inc. BET surface areas of 10.3 and 4.48 m^2/g for anatase and rutile, respectively, were measured on the Cahn RG microbalance by using nitrogen adsorption at 77 K. X-ray powder diffraction patterns of the anatase and rutile powders confirmed that the crystal structures of these materials were accurately assigned and that no phase transformations took place during the course of the experiments. Elemental analyses of impurities in the powders are reported in Table 1 (21).

The titania powders were prepared as follows. Approximately 100 mg of powder was pressed at 5000 psi for 30 min at room temperature in a 0.375 in. diameter pellet die to form a thin, approximately 0.1 in., cylindrical pellet. The sample was then loaded into the microbalance and exposed to high vacuum at room temperature. Once the base pressure was reached, the initial sample mass was measured. The sample was then exposed to 10 Torr of methanol for 60 min at room temperature. Weight gain during the methanol dose was monitored with the microbalance. After the dose was complete, the sample was exposed to high vacuum until the base pressure was reached and the saturation weight gain was then measured.Gases desorbed from the sample were monitored as the sample temperature was increased at 5 K/min until the maximum temperature of 675 K was reached. When the sample reached 675 K it was isolated from high vacuum and exposed to 10 Torr of oxygen for 60 min. The sample was slowly cooled in oxygen to room temperature,

TABLE 1

Concentration of Impurities in the TiO_2 Powders

Impurity	Anatase (% of mass)	Rutile (% of mass)
Aluminum	<0.2	<0.2
Iron	<0.2	<0.2
Phosphorus	0.2	<0.2
Halogens[a]	<0.003	0.0063

[a] Halogens calculated as chlorine.

where it was exposed to high vacuum and the final sample mass was measured. This procedure, dose–heat–oxidize, was repeated until the initial and final masses were equal and the saturation weight gain between each successive cycle was equal. Three dose–heat–oxidize cycles were requried to obtain equal saturation weight gains to within the resolution of the instrument. This treatment effectively removed physisorbed water, surface hydroxyls, chemisorbed water, and low-concentration impurities, such as chlorine. Similar treatments have been used to yield a carbonate-free and largely dehydroxylated surface (20, 22–29). Upon completion of the pellet preparation, the sample was exposed to 10 Torr of alcohol vapor at room temperature for 60 min. The weight gain of the pellet was monitored gravimetrically during alcohol exposure. This exposure has been shown to achieve chemisorption saturation coverage (20, 23, 30–32). After exposure to the alcohol, the microbalance chamber was evacuated to the base pressure and the weight gain was measured prior to initiating the temperature ramp. Upon completion of the TPD experiment, the sample was oxidized in 10 Torr of oxygen at 675 K for 1 h. The sample was allowed to cool to room temperature in oxygen. The microbalance chamber was pumped to the base pressure, and the final mass was recorded. The greatest difference between the initial and final mass for the cycle consisting of alcohol adsorption, TPD, and sample reoxidation was 10 μg, with the majority within less than 3 μg for 100-mg samples of either powder. This is an excellent indication that the oxidation treatment after the TPD effectively regenerated the initial state of the TiO_2 samples.

Infrared spectroscopy studies have shown that alcohols are dissociatively chemisorbed on titania to form alkoxides and surface hydroxyls (9, 22, 26–33). In addition to the dissociatively adsorbed alcohols, molecularly adsorbed alcohols have been reported on anatase at room temperature (9, 26–30). Molecular adsorption is likely to be minimized in this study because of the low background pressure, 5×10^{-9} Torr. Exposure to high vacuum has previously been used to remove reversibly adsorbed alcohols from anatase powders (20).

Desorption products were identified and quantified by analysis of the TPD spectra. Up to 90 selected mass fragments were monitored by rapid cycling of the mass spectrometer during the TPD experiment. The quantitative distribution of products was calculated using the method of Ko *et al.* (34) based on mass spectrometer fragmentation patterns measured with the same instrument used to collect the TPD spectra. The water yields were determined in separate experiments in which water TPD results were calibrated against microbalance measurements for water adsorption and desorption. Details of the product analysis for each of the alcohols are contained in the Appendix. The molar yields and selectivities reported below are based on the total carbon appearing in volatile products derived from surface alkoxides.

RESULTS

Uptake Measurements

The saturation coverages of the various alcohols on TiO_2 depended on both alcohol identity and bulk crystal structure of the oxide, but were quite consistent with previous reports. Uptakes at 300 K for methanol, ethanol, and 2-propanol on anatase and rutile are shown in Table 2. The saturation coverage per unit area for each alcohol was approximately 60% greater on rutile than on anatase. Since dissociative adsorption requires surface cations with at least one coordination vacancy (35), the higher capacity of rutile for alcohol adsorption implies that the rutile surface exposes more coordinatively unsaturated Ti cations per unit area than does anatase. The dependence of the uptake on alcohol structure was the same on both powders, although the amounts differed between the two powders as noted. The coverages (molecules/nm^2 catalyst) of the primary alcohols, methanol and ethanol, were approximately equal on a given powder, but that of the secondary alcohol, 2-propanol, was lower by approximately 22%. Lower saturation coverages of secondary

TABLE 2

Molecular Coverage of Alcohols on Anatase and Rutile

	Anatase			Rutile		Alcohol coverage ratio Rutile/anatase
Alcohol	This study	(20)	(36, 40)	This study	(31)	This study
Methanol	2.68	2.90	2.25	4.62	4.76	1.72
Ethanol	2.89	3.03	2.25	4.56	3.75	1.58
2-Propanol	2.22	2.32	1.85	3.49		1.57

Note. Surface areas for anatase and rutile used in this study were 10.3 and 4.48 m^2/g, respectively. All coverages are reported in molecules/nm^2.

alcohols than of primary alcohols have been observed previously and attributed to unfavorable steric interactions between branched alkoxides (20).

TPD Experiments

The reactivity of aliphatic alcohols with titania powders has been examined using a number of different techniques and pretreatments (20, 26–30, 32, 36–44). In general, alkoxide species formed by room-temperature chemisorption have been reported to leave the surface in two ways: by recombination with surface hydroxyls at approximately 400 K, and by decomposition at higher temperatures. The present results for primary and secondary alcohols also exhibited these two principal reaction channels, as described below.

2-Propanol. The adsorption and decomposition of 2-propanol on titania have been the subject of many investigations (9, 20, 22, 26, 30, 32, 36–39) and have even been used as diagnostic tools to determine the surface area of the titania component in titania–silica catalysts (37). TPD of 2-propanol produced quite similar spectra on anatase and rutile as shown in Fig. 1. The same low-temperature (ca. 410 K) desorption products, 2-propanol and water, were evolved from anatase and rutile at comparable temperatures. Likewise, the high-temperature (ca. 570 K) desorption products were identical and appeared at comparable temperatures on both powders. The relative yields of all carbon-containing products on both powders are given in Table 3. These values were calculated from the signals for individual mass fragments monitored in the TPD experiments using experimentally determined cracking patterns. The deconvolution procedures used in this study are described in the Appendix.

The product distribution and the corresponding peak temperatures shown in Table 3 are in agreement with previous investigations (20, 26, 30, 37, 39). Low-temperature peaks for 2-propanol and water occurred at the same temperature on the anatase sample (410 K), while 2-propanol (420 K) desorbed at a slightly lower temperature than water (430 K) on rutile. The low-temperature parent alcohol yield was considerably higher on anatase (40%) than on rutile (22%), i.e., the fraction converted to other products was much higher on rutile. High-temperature dehydration and dehydrogenation products, propylene and acetone, respectively, appeared at the same temperature on both powders. A high-temperature water peak appeared at a slightly lower temperature on anatase (570 K) than on rutile (580 K). On both powders the selectivity toward the dehydration product, propylene, was in excess of 90% and thus was considerably greater than that of the dehydrogenation product, acetone (8% on anatase vs. 4% on rutile). These comparisons of fractional yield and selectivity emphasize the similarity of alcohol reactivity on rutile and anatase. However, if one makes the comparison on a surface area basis by multiplying the uptakes in Table 2 by the percentage yields in Table 3, the much higher activity of rutile is apparent; more than twice as much propylene is produced per unit area of the rutile surface.

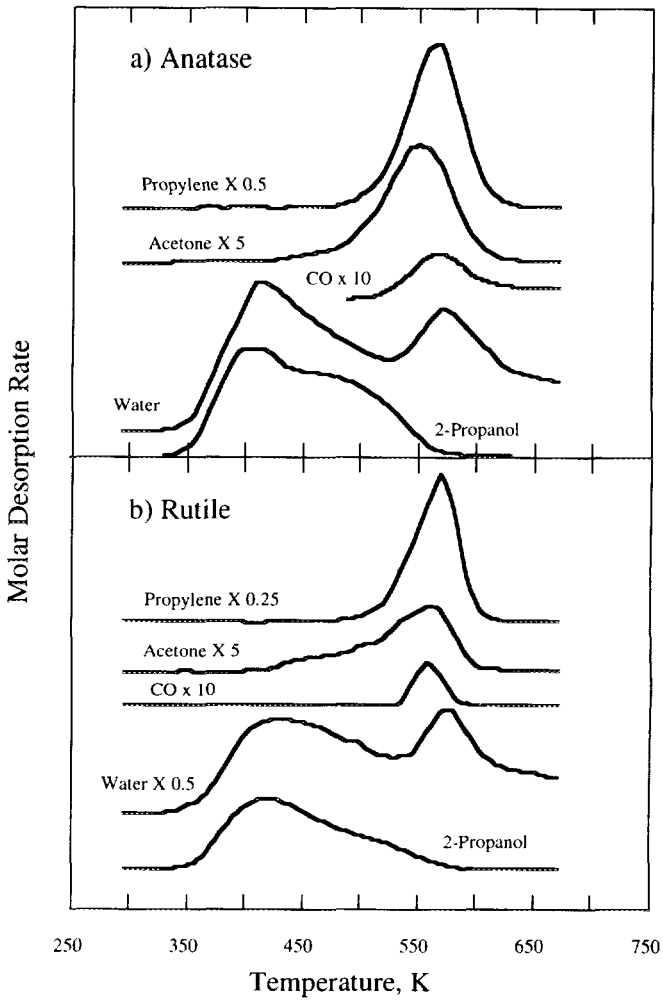

FIG. 1. TPD after 2-propanol adsorption, at room temperature, on (a) anatase and (b) rutile. Desorption peaks are offset for distinction.

There was no indication of any bimolecular reaction products, e.g., di-isopropyl ether (m/e = 87), in the TPD spectra. The absence of ether formation from secondary alcohols is consistent with previous results on anatase (20). Formation of di-isopropyl ether has been reported when 2-propanol vapor was exposed to titania (rutile) at 473 K (37), although it was not detected in the TPD of 2-propanol in the absence of vapor-phase 2-propanol (20, 26, 37). These observations suggest that ether formation from secondary alcohols requires participation of molecular alcohol species, in contrast to the coupling reactions of primary alcohols described below.

Methanol. Methanol TPD was complicated by the fact that the temperatures required for complete desorption

TABLE 3

Selectivities and Peak Temperatures of 2-Propanol TPD Products on Anatase and Rutile

Product	Peak temperature (K)		Yield (mol/100 mol alcohol adsorbed)		% Carbon selectivity	
	Anatase	Rutile	Anatase	Rutile	Anatase	Rutile
$(CH_3)_2CHOH$ (*m/e* 45 : 4.3)[a]	410	420	40	22		
C_3H_6 (*m/e* 41 : 3.6)	570	570	55	74	92	95
$(CH_3)_2CO$ (*m/e* 43 : 1.6)	555	560	4.9	3.0	8	4
CO(*m/e* 28 : 1.0)	570	560	<1	<1	<1	<1
H_2O	410	430	44	59		
H_2O	570	580	35	50		

[a] Mass spectrometer sensitivity factor and the representative fragment.

of some of the products exceeded the operating limit of the instrument. Thus, while one can obtain a reasonable measure of the selectivity to similarly affected products, the yield and conversion values are less reliable (and tend to be underestimated) than those of 2-propanol and ethanol for which complete product desorption could be achieved. TPD results for methanol on anatase and rutile are shown in Fig. 2. The same low-temperature (ca. 420 K) desorption products, methanol and water, were evolved from anatase and rutile at comparable temperatures. Previous studies have also observed methanol and water peaks at comparable temperatures to those reported here (13, 20, 26, 29, 40). Similarly, the slate of high-temperature (ca. 660 K) desorption products was the same for anatase and rutile, and these products were evolved at comparable temperatures from the two powders.

The yields and peak temperatures of all carbon-containing products are given in Table 4. The peak temperature for methanol (ca. 405 K) was below that of the low-temperature water peak (ca. 435 K) on both powders. The low-temperature water peak appeared at a lower temperature on anatase (425 K) than on rutile (455 K). The major high-temperature products desorbed in the same order with respect to temperature on both powders: dimethyl ether < formaldehyde < methane and water. The desorption of dimethyl ether appeared at a slightly lower temperature on rutile than on anatase; however, the temperature at which dimethyl ether evolved from the two samples in this study is in agreement with the temperatures reported in previous investigations (20, 28, 29, 33, 40, 41). The evolution of formaldehyde was centered at ca. 660 K and is consistent with previous studies of methanol on titania (20, 28, 29, 33, 42). Imai and Nakamura (41) studied the reactivity of methanol over hydrogen-reduced titania (773 K) and did not detect formaldehyde in the product distribution. Decomposition of formaldehyde to adsorbed carbon, adsorbed hydrogen, and lattice oxygen has been observed on reduced rutile single crystals (45). The surface oxygen deficit in such cases favors the decomposition of the alkoxide, thereby depositing oxygen on the surface. The methane desorption peak in Fig. 2 appeared at ca.

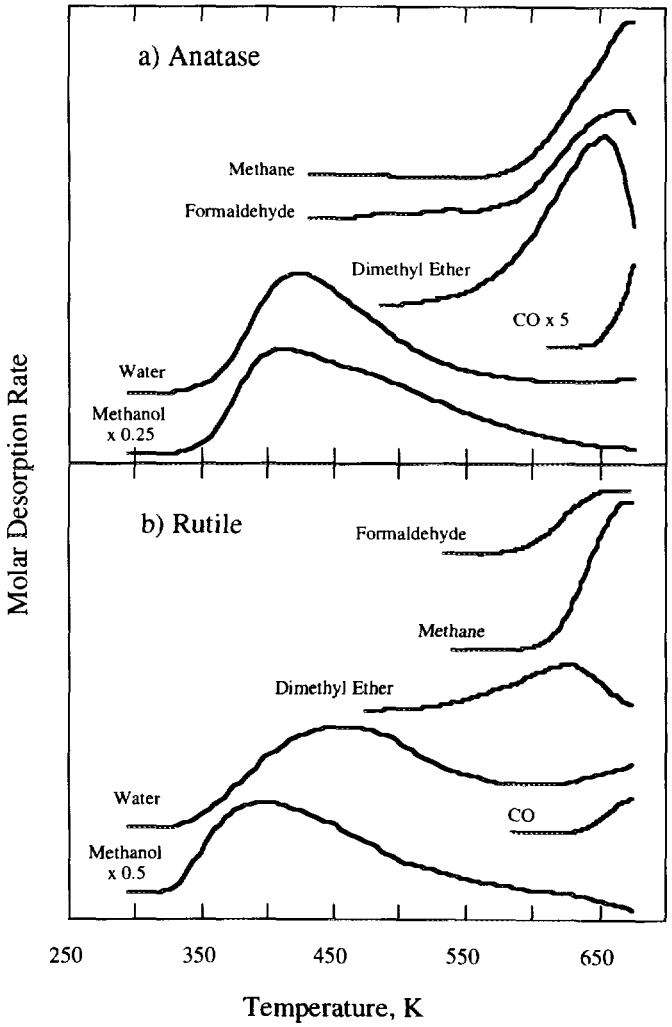

FIG. 2. TPD after methanol adsorption, at room temperature, on (a) anatase and (b) rutile. Desorption peaks are offset for distinction.

TABLE 4

Relative Selectivities and Peak Temperatures of Methanol TPD Products on Anatase and Rutile

Product	Peak temperature (K)		Yield		% Carbon selectivity	
	Anatase	Rutile	Anatase	Rutile	Anatase	Rutile
CH_3OH (*m/e* 31 : 2.7)	415	400	71	65		
CH_4 (*m/e* 16 : 1.8)	675	675	7.1	14	25	39
CH_2O (*m/e* 30 : 3.5)	660	665	7.1	9.7	25	28
$(CH_3)_2O$ (*m/e* 45 : 3.0)	655	625	6.4	4.9	45	28
CO (*m/e* 28 : 1.0)	675	675	<1	1.3	<2	3.7
CO_2 (*m/e* 44 : 1.2)	665	665	<1	<1	<2	<2
H_2O	425	455	13	37		
H_2O	675	675	1	10		

675 K, which coincided with the maximum temperature of the experimental apparatus used in this study. This peak temperature is consistent with previous studies of methanol on titania (20, 28, 29, 33, 41). As noted above, truncation of the spectra below 700 K leads to underestimates of the conversion and the product yields. It is apparent from selectivity results, however, that ether production consumes a significant fraction of the alcohol converted on both rutile and anatase, in sharp contrast to the absence of ether production from 2-propanol on either material.

Ethanol. The product distribution from ethanol was considerably richer than that from the other alcohols. TPD spectra obtained following adsorption of ethanol on anatase and rutile are shown in Fig. 3. The same desorption products were evolved from anatase and rutile at comparable temperatures. Yields and carbon selectivities for all carbon-containing products evolved are shown in Table 5.

The ethanol desorption peak (ca. 400 K) preceded the low-temperature water peak (ca. 430 K) on both powders. The low-temperature water peak appeared at a lower temperature on anatase than on rutile. Previous studies have reported water and ethanol evolution at comparable temperatures to those reported here (20, 27, 30, 44). The low-temperature parent alcohol yield was considerably higher on anatase (62%) than on rutile (34%), which is consistent with activities for 2-propanol decomposition. Therefore the conversion of surface ethoxides to products other than ethanol was greater on rutile than on anatase. The major high-temperature products desorbed in the following order with respect to temperature from the anatase sample: diethyl ether < butadiene < acetaldehyde < ethylene, ethane, butene < water. The order of the major high-temperature products was essentially the same on rutile with the exception that the acetaldehyde and butadiene temperatures were less well distinguished from each other. The evolution of each of these high-temperature products, with the exception of butadiene, has previously been reported for ethoxide decomposition on titania at

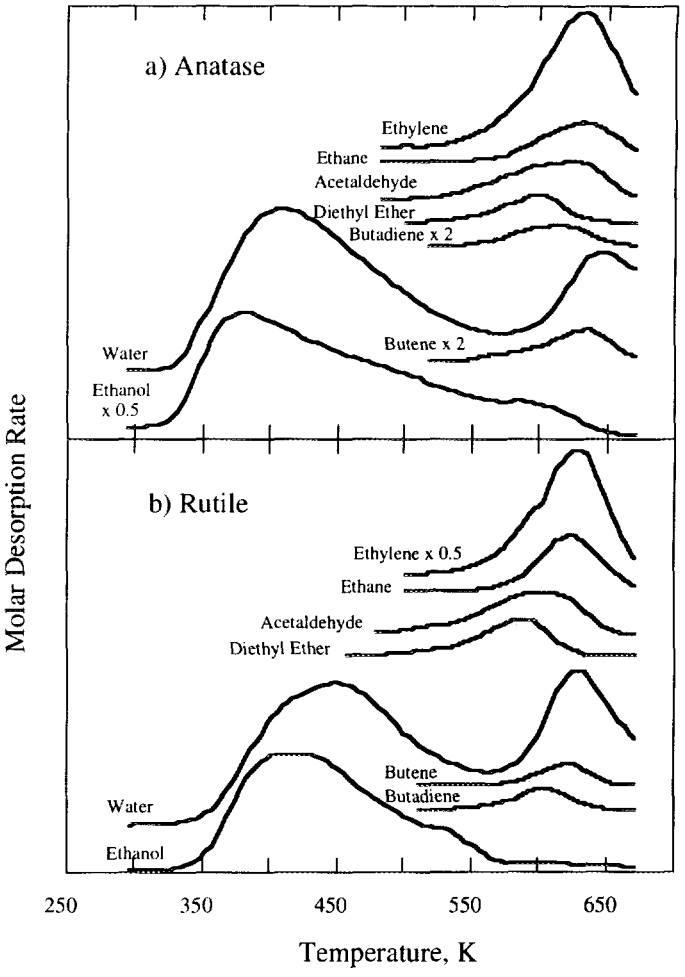

FIG. 3. TPD after ethanol adsorption, at room temperature, on (a) anatase and (b) rutile. Desorption peaks are offset for distinction.

TABLE 5

Selectivities and Peak Temperatures of Ethanol TPD Products on Anatase and Rutile

Product	Peak temperature (K)		Yield (mol/100 mol alcohol adsorbed)		% Carbon selectivity	
	Anatase	Rutile	Anatase	Rutile	Anatase	Rutile
C_2H_5OH (*m/e* 31 : 2.9)	380	415	62	34		
C_2H_4 (*m/e* 27 : 3.5)	630	625	16	33	42	50
C_2H_6 (*m/e* 30 : 5.1)	630	625	4.2	6.1	11	9.2
CH_3CHO (*m/e* 43 : 12)	620	605	6.5	8.6	17	13
$(C_2H_5)_2O$ (*m/e* 59 : 14)	600	590	2.8	4.8	15	14
C_4H_6 (*m/e* 54 : 6.1)	610	605	1.2	2.4	6.3	7.3
C_4H_8 (*m/e* 56 : 8.2)	630	625	1.5	2.0	8.2	6.2
H_2O	410	450	37	38		
H_2O	645	630	13	21		

comparable temperatures (20, 27, 30). Ethoxide species that remained on the surface of anatase and rutile decomposed at higher temperatures to produce the dehydration products ethylene, butene, butadiene, and diethyl ether, the dehydrogenation product acetaldehyde, and the hydrogenation product ethane. The most abundant product, ethylene, exhibited comparable carbon selectivities on anatase (42%) and rutile (50%), while the dehydrogenation product, acetaldehyde, was produced with lower selectivity (17% on anatase vs 13% on rutile). The sum of the carbon selectivities to bimolecular reaction products (diethyl ether, butadiene, and butene) was significant on both rutile (27.5%) and anatase (29.5%). Ether production was comparable on anatase (15%) and rutile (14%), supporting the hypothesis from the single-crystal studies that this reaction is influenced by the local cation coordination environment, and not the bulk crystal structure.

Thermal Gravimetric Analysis

Gravimetric analysis was used to measure the mass loss during alcohol TPD as well as the uptakes of alcohols during adsorption. The TGA profiles for methanol, ethanol, and 2-propanol on anatase and rutile are displayed in Fig. 4. The mass gain reported is the mass gain of the pellet after alcohol exposure and pump down to the base pressure, and corresponds to the alcohol uptakes reported in Table 2. The mass gain was normalized to a sample mass of 100.000 mg, with the actual weight of the anatase and rutile pellets being 96.509 and 100.023 mg, respectively. The primary alcohols, methanol and ethanol, exhibited similar TGA spectra, while the features of the secondary alcohol, 2-propanol, differed from the primary alcohols in the high-temperature region (>500 K) on both anatase and rutile. These data again emphasize that although the behavior of different alcohols on a given TiO_2 phase may differ, the differences for any one alcohol between the two phases of TiO_2 are small. The final mass loss was determined after the mass of the pellet remained constant for 10 min at 675 K and is reported in Table 6. The secondary alcohol produced a larger mass loss per unit area than the primary alcohols. The mass loss per unit

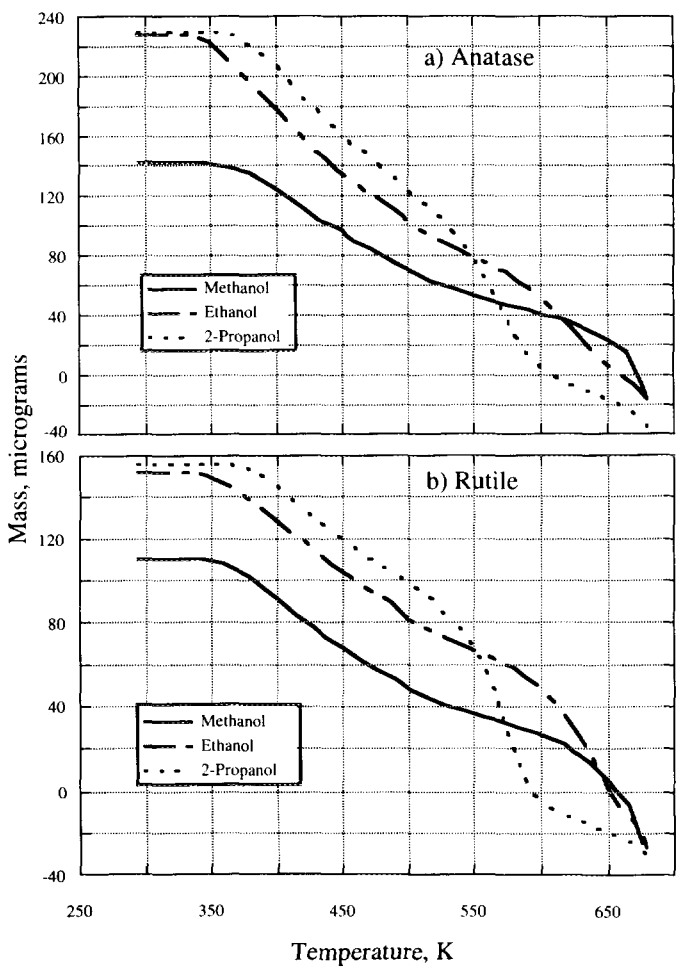

FIG. 4. TGA of the alcohols on (a) anatase and (b) rutile. The TGA was normalized to a sample mass of 100 mg.

TABLE 6

Normalized Ultimate Mass Loss on Anatase and Rutile

Alcohol	Anatase (μg)	Rutile (μg)
Methanol	17	25
Ethanol	16	27
2-Propanol	36	34

Note. Normalized to an initial sample mass of 100.00 mg. The ultimate mass loss was measured after the mass of the pellet remained constant for 10 min at 675 K and high vacuum.

area from rutile was consistent with the systematically greater conversions observed on rutile and indicated that the rutile powder surface undergoes greater reduction in the course of alcohol TPD than does anatase.

DISCUSSION

The adsorption of alcohols on titania powders has been studied extensively (9, 20, 22, 23, 26–33, 36–38, 40, 42, 44). However, a key question that none of these studies has addressed directly is the quantitative adsorption and reaction of aliphatic alcohols with pure anatase and rutile. We will therefore focus on this issue.

Alcohol adsorption on titania can be described by the sequence (11)

$$\text{R–O–H(g)} \rightarrow \text{R–O–H(ad)} \quad [1]$$

$$\text{R–O–H(g)} + \text{O(l)} \rightarrow \text{R–O(ad)} + \text{O–H(ad)}, \quad [2]$$

where O(l) represents surface lattice oxygen. Alcohols adsorb on titania both molecularly and dissociatively at room temperature (9, 22, 26–32, 36, 38, 40). Dissociative adsorption can be described as the deprotonation of alcohol at an acid-base site pair consisting of an acidic titanium cation and a basic oxygen anion. Water evolution has been reported during exposure of partially dehydroxylated rutile and anatase powders to aliphatic alcohols (26–28, 30, 31, 38). The evolution of water during alcohol adsorption has been described by the reaction sequence (26–28, 38)

$$\text{R–O–H(g)} + \text{O–H(ad)} \rightarrow \text{R–O(ad)} + \text{H}_2\text{O(g or ad)} \quad [3]$$

$$\text{R–O–H(g)} + \text{H}_2\text{O(ad)} \rightarrow \text{R–O–H(ad)} + \text{H}_2\text{O(g)}. \quad [4]$$

The evolution of water, via Eq. [4], involves displacement of molecularly adsorbed water and has been shown to be suppressed as the pretreatment temperature is increased (31). The pellet pretreatment conditions in the present case, 675 K for 60 min, produce essentially complete dehydration (22, 31) and step 4 can therefore be neglected. We have also shown previously that molecularly adsorbed alcohols are removed from anatase upon high-vacuum evacuation at 300 K (20). The uptakes reported in Table 2 are therefore based on the assignment of the entire mass gain to dissociatively adsorbed alcohols (formed by steps 2 and 3) with no products lost during adsorption.

The saturation coverages of methanol, ethanol, and 2-propanol on anatase are in agreement with previously reported values as shown in Table 2. Variations in the saturation uptake between different laboratories could be attributed to the different techniques used to measure the irreversible saturation uptake. The coverages of methanol and ethanol on anatase were 2.68 and 2.89 molecules/nm^2, respectively. The molecular coverage of 2-propanol on anatase, 2.22 molecules/nm^2, was approximately 20% lower than that of the primary alcohols, methanol and ethanol. The decreased coverage of 2-propanol relative to the primary alcohols is consistent with previous observations (20, 36, 40).

The saturation coverages of methanol and ethanol on rutile are in general agreement with previously reported values shown in Table 2, although the decrease in coverage between methanol and ethanol reported by Suda *et al.* (31) was larger than observed here. The coverages of methanol, ethanol, and 2-propanol on rutile were 4.62, 4.56, and 3.49 molecules/nm^2, respectively. The molecular coverage of 2-propanol on rutile was approximately 24% lower than that of the primary alcohols. The decreased coverage of ethanol relative to methanol reported by Suda *et al.* may reflect increased repulsive interactions due to closer adsorbate packing on rutile, as suggested by those authors (31), but it is then surprising that the decrease of the coverage of 2-propanol (24%) on rutile was not significantly greater than that on anatase (20%). Steric effects on both uptake and reaction selectivity of 2-propanol relative to primary alcohols are evident in the data presented in Tables 2–5; however, the similarity of the magnitude of these on anatase and rutile suggest that they are influenced primarily by the coordination environment of individual surface cations, rather than by surface cation density.

The numbers of surface cations exposed per unit surface area for the low index planes of anatase and rutile are given in Table 7. It has been suggested that the polycrystalline rutile surface may be represented as a 3 : 1 : 1 combination of the (110), (101), and (100) crystal planes, respectively (46), while the anatase surface may be represented as a combination of the (001), (101), and (100) crystal planes (47). The (110) plane of rutile is the most stable, exhibiting no reconstruction, possessing the highest average cation coordination number as well as the

highest cation density per unit area. One can estimate the surface cation density ratio of rutile and anatase powders either by comparing the densities of the most close-packed planes, or by applying the same 3 : 1 : 1 population ratio of low index planes for both structures. In either case, the estimated ratio of exposed Ti cations on rutile to anatase is ca. 1.5. This is essentially the same value as the average ratio of alcohol coverages on the two materials, 1.6, obtained from Table 2, and suggests that the different activities of rutile and anatase for alcohol adsorption simply reflect different areal amounts of surface Ti cations. Although this analysis in terms of only low index planes neglects the effects of edges steps, etc., present on the polycrystalline powders, the similar surface areas of the anatase and rutile samples used suggest that similar fractions of the overall surfaces are represented by such sites.

While the above results suggest that alcohol *adsorption activity* of titania powders simply reflects cation availability, studies of TiO_2 (rutile) single crystals suggest that the *selectivity* of alcohol reactions depends upon the coordination environment (extent of coordinative unsaturation) of individual surface cations. In order to consider the application of this postulate (i.e., the reactivity vs structure of TiO_2 polymorphs) it is useful to consider the pathways by which the various reaction products are formed on these materials. The results of the present study comparing rutile and anatase are generally in good agreement with previous results (20, 26–30, 33, 36–44) from studies on alcohol decomposition on one or the other of these phases. One can therefore propose a general reaction scheme to account for the various products observed in these studies, although one can also find alternative explanations for individual products suggested among these works.

Adsorbed alkoxides are removed via the low-temperature channel by recombination with surface hydroxyls, which has been previously represented by (11, 20)

$$\text{R–O(ad)} + \text{O–H(ad)} \rightarrow \text{R–O–H(g)} + \text{O(l)}. \quad [5]$$

The low-temperature water desorption can be represented as

$$2\ \text{O–H(ad)} \rightarrow \text{H}_2\text{O(g)} + \text{O(l)}. \quad [6]$$

Water desorption results in a net removal of oxygen atoms from the surface in this scheme. Molecularly adsorbed water will also desorb from the surface at low temperatures and contribute to the low-temperature water peak. Upon heating the titania surface to ca. 475 K, IR studies have shown that the surface is comprised of alkoxides and surface hydroxyls, and no molecularly adsorbed alcohols remain (9, 22, 26–29, 32, 33, 38).

When β-hydrogen atoms are present, the high-temperature reaction channel is dominated by the products of net alcohol dehydration. The reaction can be described as β-hydrogen transfer from the adsorbed alkoxide to the surface, followed by C–O bond scission to release the corresponding olefin. This chemistry has been represented (20) by

$$\text{R–O(ad)} + \text{O(l)} \rightarrow \text{O–H(ad)} + \text{R}' + \text{O(l)}, \quad [7]$$

where R′ represents a species with one less hydrogen than the alkyl group, R. The hydrogen produced during alkoxide dehydration may react with lattice oxygen to form hydroxyls, and evidence for this is provided by the high-temperature water peak in the TPD spectra of 2-propanol and ethanol. The dehydrogenation pathway is present and may be represented by (11, 20)

$$\text{R–O(ad)} \rightarrow \text{R}''\text{–O(g)} + \text{H(ad)}, \quad [8]$$

where R″ represents a ligand which has lost one alpha hydrogen from the alkyl group, R. The dehydrogenation pathway is present in the decomposition of all of the alcohols studied.

Several mechanisms have been proposed for alkane formation from alcohols. Methane evolution during methoxide decomposition was suggested to involve the readsorption of dimethyl ether and subsequent reaction of dimethyl ether to produce methane and an adsorbed formate (28, 41). An analogous mechanism for the formation of ethane during ethoxide decomposition was also proposed (27). These mechanisms are inconsistent with the production of methane in methanol TPD on rutile single crystals under UHV conditions, for which little readsorption occurs. The {011}-faceted (001) rutile surface evolved methane from methanol at 610 K, but did not produce dimethyl ether (11). If the mechanism of methane formation proceeded through the readsorption and decomposition of dimethyl ether, then dimethyl ether should have been detected in the product distribution. An alternative mechanism for methane production has been proposed (11, 20) involving filling of surface oxygen vacancies by

TABLE 7

Surface Ti Densities for the Cleavage Planes of Anatase and Rutile

Cleavage plane	Anatase (20) (Ti atoms/nm^2)	Rutile (46) (Ti atoms/nm^2)
(001)	7.0	
(101)	5.2	7.9
(110)		10.2
(100)	2.8	7.4

methoxide C–O bond scission. CH_3 species are produced by this step and decomposition of a portion of these methyl groups produces hydrogen that rapidly reacts with the remaining CH_3 groups to produce methane. When methanol and oxygen were fed over titania at 673 K, methane was not detected in the product distribution (42). Presumably the oxygen in the vapor phase maintained the surface in an oxidized state, thereby inhibiting methane production. A similar mechanism may also be used to represent the evolution of ethane during ethoxide decomposition. Small quantities of butadiene and butene evolved from both powders during ethanol TPD at approximately 610 and 630 K, respectively. Studies performed on partially reduced rutile single crystals have reported carbonyl metathesis to form higher olefins (48). The presence of small amounts of the reductive coupling products, butene and butadiene, suggests that the surface of the titania was slightly reduced. The peaks for these products were within the envelope of that for the dehydrogenation product, acetaldehyde, consistent with the suggestion that a small amount of the acetaldehyde produced is reductively coupled to form these products.

The one reaction that has been shown to be sensitive to surface structure in single-crystal studies on TiO_2 is the bimolecular dehydration of alcohols to form ethers. This reaction involves coupling of a pair of alkoxides and can be represented as (11, 20, 33)

$$2\ \text{R–O(ad)} \rightarrow \text{R–O–R(g)} + \text{O(l)}. \qquad [9]$$

The reaction of methoxy species on the {114}-faceted (001) surface of rutile, which exposes doubly coordinatively unsaturated surface cations, has been shown to produce dimethyl ether, in contrast to the {011}-faceted (001) surface which exposes only singly coordinatively unsaturated surface cations, and does not produce dimethyl ether (11). The evolution of dimethyl ether and diethyl ether from both rutile and anatase polymorphs of titania in the present study implies that both powders expose doubly coordinatively unsaturated surface cations. The relative populations of doubly coordinatively unsaturated cations on each material are approximately equivalent, based upon the agreement in selectivities for diethyl ether production. Diethyl ether selectivities on the two polymorphs were essentially indistinguishable: 15% on anatase vs 14% on rutile. The yield of diethyl ether per unit area was significantly greater on rutile (0.44 ethoxide/nm^2) than on anatase (0.16 ethoxide/nm^2), reflecting the higher conversions and larger uptakes of ethanol on rutile. The absence of di-isopropyl ether from 2-propanol decomposition is expected since the greater steric inhibition of the branched alkoxide prevents attachment of two ligands to a common cation site, and is also consistent with the decreased saturation coverage of the secondary alcohol relative to the primary alcohols.

Multiply unsaturated cations on titania surfaces have been invoked in previous work to explain particular reaction channels that showed anatase/rutile differences. For example, Beck *et al.* reported that rutile catalytically decomposed hydrogen sulfide, but anatase did not (7). They proposed the active site for decomposition to be adjacent five- and four-coordinate titanium cations with neighboring lattice oxygen or hydroxyl groups on the (110) plane of rutile. In a related publication, Beck *et al.* (8) reported differences in the TPD of oxygen and carbon monoxide from anatase and rutile and suggested that in general the "distinctive surface chemistry" of rutile compared to anatase is derived from adjacent four- and five-coordinated titanium atoms on the (110) plane of rutile. If the (110) plane of rutile is defect free, the surface cations have six- and fivefold coordination to oxygen anions (49). The model suggested by Beck *et al.* assumes that the rutile surface has undergone a significant degree of reduction, while the anatase surface remains oxidized. In contrast, Ramis *et al.* (9) reported dissociative and molecular chemisorption of aliphatic alcohols at room temperature on anatase and only dissociative chemisorption on rutile. Ramis *et al.* postulated that molecular adsorption occurred on doubly unsaturated surface cations exposed on the (110) plane of anatase, while rutile only supported dissociative adsorption because it only exposed singly unsaturated surface cations. In this study we have determined, on the basis of alcohol reaction selectivities established for coordinatively unsaturated cations on single crystal surfaces, that both polymorphs expose doubly unsaturated surface cations, even when oxidized, and that their chemistry is remarkably similar.

TGA spectra corroborated the product evolution measured with TPD. The ultimate mass loss per unit surface area from rutile was greater than anatase for all of the alcohols studied. Activation energies for catalytic oxidation of hydrogen and carbon monoxide, and the catalytic decomposition of nitrous oxide are lower on rutile than anatase (50–52), which suggests that rutile is more likely to become oxygen deficient than anatase. Therefore the increased mass loss for rutile, relative to anatase, is presumably due to the enhanced reducibility of rutile, if one assumes that the ultimate mass loss represents the number of oxygen vacancies produced during the adsorption and decomposition of aliphatic alcohols. The greater ease of reduction of rutile may be manifested in its ease in forming water, via Eq. [3], instead of preserving hydroxyl groups for recombination with alkoxides. The higher yield of the parent alcohols from anatase indicated that more surface hydroxyls recombined with alkoxides. Furthermore, the water yield was consistently higher on rutile than anatase for each alcohol studied, and the fraction of the adsorbed alkoxides converted to products via the high-temperature reaction channels was correspondingly greater on rutile.

Although bulk structure and the surface cation density of anatase and rutile differ appreciably, there are relatively few differences in the surface chemistry of oxygenates on these polymorphs, consistent with the proposal that this chemistry is largely controlled by the local coordination environment of individual surface cations. The similar character of these two materials is further supported by comparing the energetics of the various surface reaction processes. The peak temperatures corresponding to the high-temperature products were within 15 K on both powders for all of the products, with the exception of dimethyl ether. Peak widths for like products on anatase and rutile were also similar, as is apparent from Figs. 1–3, suggesting that the pre-exponential factors for the various surface reactions on the two materials are comparable. Given the similar surface areas of the materials studied, diffusion effects should also be similar. Thus, the agreement of peak temperatures in TPD experiments is an excellent indication that the energetics of the reactions occurring on the different powder surfaces are comparable.

The absence of an effect of the bulk structure of oxide polymorphs on surface alkoxide chemistry has previously been demonstrated on the α- and β-phases of MoO_3 by Farneth *et al.* (53). The α-phase is characterized by a layered orthorhombic structure, which gives rise to platelike crystallites dominated by the basal plane; this surface exposes *no* coordinatively unsaturated cations. Methanol uptakes per total unit area of this material reflect the fact that methanol is dissociatively adsorbed only on the cations exposed by the apical and side planes (53). The structure of the monoclinic β-phase, in contrast, gives rise to surfaces on which each cation has a single coordination vacancy, and for which quantitative uptakes for a series of oxygenated compounds, including methanol, ethanol, and 2-propanol, are consistently greater than the α-phase (53). On the basis of gross surface area, these two polymorphs of MoO_3 exhibit a significant difference in alcohol capacity, similar to those of TiO_2 examined in the present study. Like the TiO_2 example considered here, once one accounts for different uptake capacities, the reactivities of the two MoO_3 polymorphs are quite similar, both with respect to product selectivities and reaction energetics (53). For both TiO_2 and MoO_3 polymorphs, therefore, it is the coordination environment of individual surface cations that controls surface reactivity, and not the bulk crystal structure.

The results of this study of alcohol decomposition demonstrate that the principal difference between rutile and anatase surfaces is the population of surface cations. The low index planes of rutile are characterized by surface cation densities ca. 50% higher than those of comparable anatase samples, and the capacity for alcohol dissociation of these two polymorphs reflects that ratio almost stoichiometrically. The characteristics of these sites on anatase and rutile are quite similar, both product distributions and reaction and desorption kinetics are in excellent agreement. Selectivities for bimolecular coupling of alkoxides to form ethers are also in good agreement, suggesting that the fraction of multiply coordinatively unsaturated cations on rutile and anatase powders is approximately the same. This observation is perhaps not surprising, since for comparable surface area powders, one has comparable crystallite sizes and one would expect comparable populations of multiply coordinatively unsaturated sites arising at edges, corners, grain boundaries, etc. The key point, however, is that while bimolecular coupling to form ethers exhibits a clear dependence on cation coordination environment in single-crystal studies, it is not affected by changes in bulk structure which do not alter the coordination of individual surface cations. The results of this study on high-surface-area TiO_2 powders are thus entirely consistent with site requirements for unimolecular and bimolecular reactions of alcohols determined from studies on well-defined single-crystal surfaces.

CONCLUSIONS

The site requirements for unimolecular and bimolecular reaction of alcohols, deduced from studies performed on rutile single crystals, are sufficient to account for the reactivity on polycrystalline anatase and rutile powders. Both polymorphic forms produced dialkyl ethers from the primary alcohols studied, which is indicative of the presence of doubly unsaturated surface cations on both powder surfaces. The principal activity difference between rutile and anatase reflects the population of surface cations per unit area. This is manifested in the uptake measurements, where rutile gave rise to greater alcohol coverages than did anatase for each of the alcohols studied; the ratios of the coverages were consistent with the ratio of surface cation populations on the two polymorphs. The reaction behavior of surface cations on the two polymorphs could be explained solely in terms of individual cation coordination environment. The reactions of each of the alcohols studied on anatase and rutile produced identical products, with comparable selectivities and with similar energetics on the two materials. This demonstrates that the chemistry of alcohols on titania is determined by local coordination and not by the bulk-crystal structure.

Decreased adsorption of secondary alcohols relative to primary alcohols was observed on rutile, and is consistent with previous results on anatase. The increased hindrance of the isopropoxide derived from 2-propanol appears to be sufficient to prevent two alkoxides from bonding to the same doubly coordinatively unsaturated cation, thereby preventing the formation of di-isopropyl ether. This obser-

vation provides additional support for the site requirement for etherification deduced from single-crystal studies.

APPENDIX

The product assignments and distributions were resolved through the analysis of TPD mass spectra. The details of the product deconvolution are given below for the alcohols studied.

2-Propanol

1. The areas under each peak for m/e = 45, 44, 43, 42, 41, 40, 29, 28, 27, 26, 18, and 15 were obtained by numerical integration.
2. The fragmentation patterns for 2-propanol and water were scaled to account for the entire m/e = 45 and 18 signals, respectively, and subtracted from the peak area of each mass.
3. The fragmentation patterns for acetone and propylene were scaled to account for the remaining m/e = 43 and 41 signals, respectively, and subtracted from the peak area of each mass.
4. The fragmentation pattern for carbon monoxide was scaled to account for the remaining m/e = 28 signal.
5. The amounts of each product were determined from the peak area deconvolution above using mass spectrometer sensitivity factors calculated from the measured cracking patterns (34). Selectivities were normalized with respect to the carbon number of each product and reflect the fraction of the total carbon converted to products that appears in each product. The RMS percentages of the TPD peak areas, positive or negative, remaining at the end of this procedure were 1.8 and 1.5, for 2-propanol TPD from rutile and anatase, respectively, based on the 10 most abundant masses. The remaining intensity of the m/e = 44 signal was extremely small, thus the amounts of carbon dioxide and propane formed were negligible.

Methanol

1. The area under each peak for m/e = 46, 45, 44, 43, 32, 31, 30, 29, 28, 18, 16, and 15 was obtained by numerical integration of the TPD spectra up to 675 K.
2. The fragmentation patterns for dimethyl ether and water were scaled to account for the entire m/e = 45 and 18 signals, respectively, and subtracted from the peak area of each mass.
3. The fragmentation pattern for carbon dioxide was scaled to account for the remaining m/e = 44 signal and subtracted from the remaining peak area of each mass.
4. The fragmentation pattern for methanol was scaled to account for the remaining m/e = 31 signal and subtracted from the remaining peak area of each mass.
5. The fragmentation pattern for formaldehyde was scaled to account for the remaining m/e = 30 signal and subtracted from the remaining peak area of each mass.
6. The fragmentation pattern for carbon monoxide was scaled to account for the remaining m/e = 28 signal and subtracted from the remaining peak area of each mass.
7. The fragmentation pattern for methane was scaled to account for the remaining m/e = 16 signal and subtracted from the peak area of m/e = 15.
8. The relative yields and carbon selectivities of each product were determined using calculated mass spectrometer sensitivity factors. The RMS percentages of TPD peak areas remaining at the end of this procedure were 1.5 and 0.6 for methanol TPD from rutile and anatase, respectively, based on the 10 most abundant masses. Ethane and ethylene could be excluded from the product distribution because there was no detectable intensity for m/e = 26 and 27.

Ethanol

1. The area under each peak for m/e = 78, 74, 59, 56, 55, 54, 53, 45, 44, 43, 42, 41, 39, 31, 30, 29, 28, 27, 26, 18, 15, and 14 was obtained by numerical integration.
2. The fragmentation patterns for diethyl ether, butene, butadiene, and water were scaled to account for the entire m/e = 59, 56, 54 and 18 signals, respectively, and subtracted from the peak area of each mass.
3. The fragmentation pattern for ethanol was scaled to account for the remainder of the m/e = 31 signal and subtracted from the peak area of each mass.
4. The fragmentation pattern for acetaldehyde was scaled to account for the remainder of the m/e = 43 signal and subtracted from the peak area of each mass.
5. The fragmentation pattern for ethane was scaled to account for the remainder of m/e = 30 signal and subtracted from the peak area of each mass.
6. The fragmentation pattern for ethylene was scaled to account for the remainder of the m/e = 27 signal and subtracted from the peak area of each mass.
7. The yields for each product were determined using calculated mass spectrometer sensitivity factors. Carbon selectivities were normalized with respect to the carbon content of each of the reaction products. The RMS percentages of TPD peak areas remaining at the end of this procedure were 5.7 and 9.0, for ethanol TPD from rutile and anatase, respectively, based on the 20 most abundant masses. The intensities of the m/e = 44 and 28 signals remaining after subtraction of the contributions from the organic products above were extremely small, and therefore the amounts of carbon dioxide and carbon monoxide were taken to be negligible. Trace quantities of benzene (m/e = 78 and 77) were detected at high temperatures (ca. 650 K). Crotyl alcohol (m/e = 72 and 57) and crotonaldehyde (m/e = 70 and 69), the aldol condensation prod-

ucts of acetaldehyde (55), could be excluded from the product distribution because there was no detectable intensity for their representative fragments.

ACKNOWLEDGMENTS

We gratefully acknowledge the National Science Foundation (Grant CTS 9100404) and E. I. duPont de Nemours & Co., Inc. for support of this research. We also thank Willis Dolinger for his very capable technical assistance.

REFERENCES

1. Parfitt, G. D., *in* "Progress in Surface and Membrane Science (D. A. Cadenhead and J. F. Danielli, Eds.), Vol. 11, p. 181. Academic Press, New York, 1976.
2. Rao, C. N. R., Yoganarasimhan, S. R., and Faeth, P. A., *Trans. Faraday Soc.* **57,** 504 (1961).
3. Yoganarasimhan, S. R., and Rao, C. N. R., *Trans. Faraday Soc.* **58,** 1579 (1962).
4. Rao, C. N. R., *Can. J. Chem.* **39,** 498 (1961).
5. Czanderna, A. W., Rao, C. N. R., and Honig, J. M., *Trans. Faraday Soc.* **54,** 1069 (1958).
6. Ziolek, M., Kujawa, J., Saur, O., and Lavalley, J. C., *J. Phys. Chem.* **97,** 9761 (1993).
7. Beck, D. D., White, J. M., and Ratcliffe, C. T., *J. Phys. Chem.* **90,** 3123 (1986).
8. Beck, D. D., White, J. M., and Ratcliffe, C. T., *J. Phys. Chem.* **90,** 3132 (1986).
9. Ramis, G., Busca, G., and Lorenzelli, V., *J. Chem. Soc., Faraday Trans. I* **83,** 1591 (1987).
10. Rives, A. B., Kulkarni, T. S., and Schwaner, A. L., *Langmuir* **9,** 192 (1993).
11. Kim, K. S., and Barteau, M. A., *Surf. Sci.* **223,** 13 (1989).
12. Kurtz, R. L., *Surf. Sci.* **177,** 526 (1986).
13. Firment, L. E., *Surf. Sci.* **116,** 205 (1982).
14. Kim, K. S., and Barteau, M. A., *J. Mol. Catal.* **63,** 103 (1990).
15. Kim, K. S., and Barteau, M. A., *J. Catal.* **125,** 353 (1990).
16. Idriss, H., Kim, K. S., and Barteau, M. A., *in* "Structure-Activity and Selectivity Relationships in Heterogeneous Catalysis" (R. K. Grasselli and A. W. Sleight, Eds.), p. 327. Elsevier, Amsterdam, 1991.
17. Kim, K. S., and Barteau, M. A., *Langmuir* **4,** 945 (1988).
18. Onishi, H., Aruga, T., and Iwasawa, Y., *J. Catal.* **146,** 557 (1994).
19. Farneth, W. E., Ohuchi, F., Staley, R. H., Chowdury, U., and Sleight, A. W. *J. Phys. Chem.* **89,** 2493 (1985).
20. Kim, K. S., Barteau, M. A., and Farneth, W. E. *Langmuir* **4,** 533 (1988).
21. Galbraith Laboratories, Inc., Knoxville, Tennessee.
22. Boaventura, J. S., Ph.D. Dissertation, University of Delaware (1989).
23. Hollabaugh, C. M., and Chessick, J. J., *J. Phys. Chem.* **65,** 109 (1961).
24. Jackson, P., and Parfitt, G. D., *Trans. Faraday Soc.* **67,** 2469 (1971).
25. Jones, P., and Hockey, J. A., *Trans. Faraday Soc.* **67,** 2669 (1971).
26. Hussein, G. A. M., Sheppard, N., Zaki, M. I., and Fahim, R. B., *J. Chem. Soc. Faraday Trans.* **85,** 1723 (1989).
27. Hussein, G. A. M., Sheppard, N., Zaki, M. I., and Fahim, R. B., *J. Chem. Soc. Faraday Trans.* **87,** 2655 (1991).
28. Hussein, G. A. M., Sheppard, N., Zaki, M. I., and Fahim, R. B., *J. Chem. Soc. Faraday Trans.* **87,** 2661 (1991).
29. Busca, G., Forzatti, P., Lavalley, J. C., and Tronconi, E., *in* "Catalysis by Acids and Bases" (B. Imelik, C. Naccache, G. Coudurier, Y. Ben Taarit, and J. C. Vedrine, Eds.), p. 15. Elsevier, Amsterdam, 1985.
30. Munuera, G., and Carrizosa, I., *J. Catal.* **49,** 174 (1977).
31. Suda, Y., Morimoto, T., and Nagao, M., *Langmuir* **3,** 99 (1987).
32. Rossi, P. F., Busca, G., Lorenzelli, V., Saur, O., and Lavalley, J. C., *Langmuir* **3,** 52 (1987).
33. Taylor, E. A., and Griffin, G. L., *J. Phys. Chem.* **92,** 477 (1988).
34. Ko, E. I., Benziger, J. B., and Madix, R. J., *J. Catal.* **62,** 264 (1980).
35. Barteau, M. A., *J. Vac. Sci. Technol. A.* **11,** 2162 (1993).
36. Carrizosa, I., and Munuera, G., *J. Catal.* **49,** 189 (1977).
37. Biaglow, A. I., Gorte, R. J., Srinivasan, S., and Datye, A. K., *Catal. Lett.* **13,** 133 (1992).
38. Rochester, C. H., Graham, J., and Rudham, R., *J. Chem. Soc., Faraday Trans. I* **80,** 2459 (1984).
39. Gentry, S. J., Rudham, R., and Wagstaff, K., *J. Chem. Soc., Faraday Trans. I* **71,** 657 (1975).
40. Carrizosa, I., Munuera, G., and Castanar, S., *J. Catal.* **49,** 265 (1977).
41. Imai, H., and Nakamura, K., *J. Catal.* **125,** 571 (1990).
42. Groff, R. P., and Manogue, W. H., *J. Catal.* **87,** 461 (1984).
43. Groff, R. P., and Manogue, W. H., *J. Catal.* **79,** 462 (1983).
44. Jackson, P., and Parfitt, G. D., *Trans. Faraday Soc.* **68,** 1443 (1972).
45. Idriss, H., Kim, K. S., and Barteau, M. A., *Surf. Sci.* **262,** 113 (1992).
46. Jones, P., and Hockey, J. A., *Trans. Faraday Soc.* **67,** 2679 (1971).
47. Tanaka, K., and White, J. M., *J. Phys. Chem.* **85,** 4708 (1982).
48. Idriss, H., Pierce, K., and Barteau, M. A., *J. Am. Chem. Soc.* **113,** 715 (1991).
49. Henrich, V. E., *Rep. Prog. Phys.* **48,** 1481 (1985).
50. Onishi, Y., *Bull. Chem. Soc. Jpn.* **44,** 912 (1971).
51. Onishi, Y., *Bull. Chem. Soc. Jpn.* **44,** 1460 (1971).
52. Onishi, Y., *Bull. Chem. Soc. Jpn.* **45,** 922 (1972).
53. Farneth, W. E., McCarron, E. M., III, Sleight, A. W., and Staley, R. H., *Langmuir* **3,** 217 (1987).
54. Farneth, W. E., Staley, R. H., and Sleight, A. W., *J. Am. Chem. Soc.* **108,** 2327 (1986).